

Supplementary Materials

Near-canopy horizontal concentration heterogeneity of semivolatile oxygenated organic compounds and implications for primary emissions

Jianhuai Ye* (1), Carla E. Batista (2,3), Patricia C. Guimarães (2,3), Igor O. Ribeiro (2,3), Charles Vidoudez (4), Rafael G. Barbosa (3), Rafael L. Oliveira (3), Yongjing Ma (1, 5), Kolby J. Jardine (6), Jason D. Surratt (7), Alex B. Guenther (8), Rodrigo A. F. Souza (2,3), Scot T. Martin* (1,9)

(1) School of Engineering and Applied Sciences, Harvard University, Cambridge, Massachusetts, 02138, USA

(2) Post-graduate Program in Climate and Environment, National Institute of Amazonian Research, Manaus, Amazonas, 69060-001, Brazil

(3) School of Technology, Amazonas State University, Manaus, Amazonas, 69065-020, Brazil

(4) Harvard Center for Mass Spectrometry, Harvard University, Cambridge, Massachusetts, 02138, USA

(5) College of Atmospheric Sciences, Lanzhou University, Lanzhou, 730000, China

(6) Climate and Ecosystem Sciences Division, Earth Science Division, Lawrence Berkeley National Laboratory, Berkeley, California, 94720, USA

(7) Department of Environmental Sciences and Engineering, Gillings School of Global Public Health, University of North Carolina at Chapel Hill, Chapel Hill, North Carolina, 27599, USA

(8) Department of Earth System Science, University of California, Irvine, California, 92697, USA

(9) Department of Earth and Planetary Sciences, Harvard University, Cambridge, Massachusetts, 02138, USA

Correspondence to: Scot T. Martin (scot_martin@harvard.edu), ORCID: 0000-0002-8996-7554.
Jianhuai Ye (jye@seas.harvard.edu), ORCID: 0000-0002-9063-3260

Text S1. Gradient Transport Model

A two-dimensional gradient transport model was used to examine factors that might influence the spatial heterogeneity of SV-OVOC concentrations. Details of the model are described in Batista et al. (1). Briefly, the gradient transport model resolves atmospheric chemical transport and mass transfer by taking into consideration emission and deposition, longitudinal advection, vertical convection, and chemical reactions of VOCs and SV-OVOCs, represented in Equation 1. The domain size was $100 \times 1.0 \times 0.1 \text{ km}^3$ (longitudinal \times vertical \times transversal), and the corresponding resolution was $0.1 \times 0.02 \times 0.1 \text{ km}^3$. A longitudinal limit of 100 km was sufficient such that the species concentrations reached a steady state at the point sampled in the simulation. A vertical height of 1.0 km corresponded to the typical daytime boundary layer heights over the tropical forest. Transverse mixing was unimportant for the prevailing wind speeds, and for simplification it was therefore omitted from the treatment. Boundary conditions of $C = 0$ were used for the upwind limit ($x = 100 \text{ km}$) and the vertical limit ($z = 1.0 \text{ km}$). Emissions from the forest were simulated for the other vertical limit ($z = 0.0 \text{ km}$). The parameter values of Equation 1 that were used in the simulation are listed in Tables 1 and S3. These values, except for the primary emission rates of 2-methyltetrols, were either measured during the sampling or obtained from the literature for the same region (i.e., the central Amazon).

Text S2. Heterogeneous Distribution of Oxidant Concentration

A heterogeneous distribution of oxidant concentration, especially that of the short-lived atmospheric hydroxyl radical (OH), can cause spatial heterogeneities in the production of SV-OVOCs. Santos et al. (2) demonstrated that the oxidation of isoprene can differ by a factor of

four inside and outside of fresh smoke because of differences in OH concentration. The spatial heterogeneity in oxidants and VOCs can result in spatial heterogeneity of reaction rates. Accounting for reaction rates in each segregated pocket and subsequently averaging reaction rates across these pockets (i.e., corresponding to real atmospheric processes) can lead to net reaction rates that are significantly different than assuming average concentrations and then calculating reaction rates. For example, Butler et al. (3) demonstrated that the modeled reaction rate between isoprene and OH was 50% too fast in order to match isoprene concentrations observed during a campaign over a tropical forest. Agreement was possible, however, by including in the simulation the heterogeneity of isoprene and OH concentrations throughout the mixed layer.

Text S3. 2-Methyltetrols Organosulfates

2-Methyltetrols organosulfates were observed to constitute a significant or dominant fraction of the 2-methyltetrols family, at least in the particle phase in the central Amazon (4, 5). The occurrence of high concentrations of 2-methyltetrols organosulfates in the particle phase implies that secondary production takes place and that concentrations may accumulate across several days given their atmospheric lifetimes (6). Based on this timescale, this mechanism, if considered in isolation of other factors, implies that homogeneous rather than heterogeneous concentrations would be observed across the study scale of 1000 m between locations P and S. The observations show the opposite behavior. A strong local source of direct emissions is needed to explain the results, as discussed in section, “Non-uniform VOC emission rates,” in the main text.

Table S1. Meteorological parameters measured at the top of the tower during the four weeks of sampling. The indicated values are means across 09:00 and 13:30 (local time) during the sampling days. The quantities appearing after “±” indicate the one-sigma variations during the sampling periods.

	Dates	Dominant Winds	Wind Speed (m s ⁻¹)	Temperature (°C)	Relative Humidity (%)
Week 1	21 Feb 2018–27 Feb 2018	easterlies, northeasterlies	1.2 ± 0.9	26.4 ± 1.6	86.9 ± 7.3
Week 2	28 Feb 2018–05 Mar 2018	easterlies	1.9 ± 0.8	28.9 ± 1.7	79.7 ± 9.6
Week 3	06 Mar 2018–10 Mar 2018	northeasterlies	1.9 ± 1.0	27.6 ± 1.4	86.8 ± 5.3
Week 4	12 Mar 2018–15 Mar 2018	northeasterlies	2.0 ± 1.1	27.0 ± 1.5	87.6 ± 7.5
Ensemble Mean			1.8 ± 1.0	27.4 ± 1.6	85.3 ± 7.4

Table S2. Concentrations of SV-OVOC species for each hourly sampling period of each week. The listed species are oxidation products of isoprene and monoterpenes. The overall uncertainty of each concentration was <30%. The listed values are plotted in Figure 2A and Figure S2. “P” and “S” refer to locations P and S (Figure 1B). The values represent total concentrations including both gas- and particle-phase concentrations. “N/D” indicates that the species concentration was below the limit of detection. *Percent difference in the concentration at location S relative to that at location P.

Time	Pinonic Acid (ng m ⁻³)			Pinic Acid (ng m ⁻³)			2-Methyltetrols (ng m ⁻³)			2-Methylthreitol (ng m ⁻³)		2-Methylerythritol (ng m ⁻³)	
	P	S	Δ (%)*	P	S	Δ (%)*	P	S	Δ (%)*	P	S	P	S
Week 1													
09:00–10:00	7	/		19	/		134	/		56	/	79	/
10:10–11:10	8	N/D		N/D	N/D		170	148	-13	72	56	98	92
11:20–12:20	8	9	+7	21	26	+24	145	123	-15	53	54	92	69
12:30–13:30	11	13	+18	N/D	21		149	115	-23	60	46	89	69
Weekly Mean	9	11	+22	20	24	+20	150	129	-14				
Week 2													
09:00–10:00	9	11	+22	12	10	-17	113	195	+73	47	79	66	116
10:10–11:10	11	13	+18	12	14	+17	335	469	+40	120	168	215	301
11:20–12:20	13	16	+23	15	14	-7	117	501	+328	47	179	70	323
12:30–13:30	12	15	+25	13	16	+23	132	760	+476	57	249	74	511
Weekly Mean	11	14	+27	13	14	+8	174	481	+176				
Week 3													
09:00–10:00	56	53	-5	50	58	+16	315	286	-9	115	100	200	186
10:10–11:10	52	62	+19	117	138	+18	274	290	+6	98	117	176	173
11:20–12:20	64	80	+25	170	141	-17	461	453	-2	150	142	310	311
12:30–13:30	63	73	+16	196	184	-6	143	477	+234	51	176	92	301
Weekly Mean	59	67	+14	133	130	-2	298	377	+27				
Week 4													
09:00–10:00	48	51	+6	60	/		547	392	-28	172	135	375	258
10:10–11:10	63	71	+13	65	/		848	292	-66	271	94	577	198
11:20–12:20	57	58	+2	52	46	-12	375	681	+82	119	210	256	471
12:30–13:30	55	58	+5	44	48	+9	768	1006	+31	273	308	495	698
Weekly Mean	56	60	+7	55	47	-15	635	593	-7				

Table S3. Parameter values for Equation 1 for the sensitivity analysis. Values in the parentheses are used in the reference simulation. *The reaction rate of 2-methyltetrols is taken as the same as that of erythritol due to similar chemical structures. †The wind speed at altitude z was estimated using the relationship: $u(z) = (u^f / \kappa_v) \ln[(z - d) / z_0]$. Symbols include u^f as the friction velocity (0.25, Ref. (1)), κ_v as the von Kármán constant (0.40), z_0 as the roughness length (1/30 of the canopy height), and d as the displacement height (3/4 of the canopy height). A canopy height of 30 m was used.

Symbol	Quantity	Value	Units	Source
$k_{\text{ISO+OH}}$	Reaction rate constant of isoprene with OH	1.0×10^{-16}	$\text{m}^3 \text{ molec}^{-1} \text{ s}^{-1}$	Ref. (7)
$k_{\text{ISO+O}_3}$	Reaction rate constant of isoprene with O ₃	1.3×10^{-23}	$\text{m}^3 \text{ molec}^{-1} \text{ s}^{-1}$	Ref. (7)
$k_{\text{2MT+OH}}$	Reaction rate constant of 2-methyltetrols with OH	$2.5 \times 10^{-19*}$	$\text{m}^3 \text{ molec}^{-1} \text{ s}^{-1}$	Ref. (8)
y	Chemical yield of 2-methyletrols	0.6%		Ref. (9); based on chamber studies
[OH]	Hydroxyl radical concentration	0.2 to 11 (6.0) $\times 10^{12}$	molec m^{-3}	Ref. (1) and Ref (2)
[O ₃]	Ozone concentration	2.5 to 5.0 (3.0) $\times 10^{17}$	molec m^{-3}	Ref. (1) and Ref (10)
τ_{ISO}	Isoprene lifetime against chemical loss	15 to 700 (30)	min	$(k_{\text{ISO+OH}} [\text{OH}] + k_{\text{ISO+O}_3} [\text{O}_3])^{-1}$
τ_{2MT}	2-methyletrols lifetime against chemical loss	4 to 230 (8)	day	$(k_{\text{2MT+OH}} [\text{OH}])^{-1}$
u	Horizontal wind speed (advection)	1.8	m s^{-1}	Average value measured at location A during sampling (Table S1)
		2.5	m s^{-1}	Estimated at 50 m above canopy [†]
K	Eddy diffusion coefficient at top of canopy	30	$\text{m}^2 \text{ s}^{-1}$	Ref. (1)

Table S4. Literature summary of 2-methyltetrols concentrations for the Amazon region. The 2-methyltetrols concentration is the sum of 2-methylthreitol concentration and the 2-methylerythritol concentration. The concentration ratio of these latter two species is also listed in the table. The quantity appearing after “±” indicates the one-sigma variation during the sampling period. Related notes about concentration appear in the caption of Table S2. *The ratios were calculated based on the average particle fractions of 2-methylthreitol and 2-methylerythritol (0.31 and 0.55, respectively) in the wet season of the central Amazon (5). †The particle-phase 2-methyltetrols concentration only was reported in the literature.

Site	Air Quality Conditions	Season	2-Methyltetrols (ng m ⁻³)	$\frac{[2\text{-methylthreitol}]_{\text{particle}}}{[2\text{-methylerythritol}]_{\text{particle}}}$	Reference
Ducke Reserve (forest), central Amazon, northern outskirts of Manaus	Polluted	Wet season	314 ± 234	0.34 ± 0.06*	This study (location P)
		Wet season	413 ± 253	0.32 ± 0.06*	This study (location S)
T3 site (rural), central Amazon, 70 km to the west of Manaus	Polluted	Wet season	25–325	0.31	Ref. (5) and Ref. (11)
ZF2 site (forest), central Amazon, 60 km to the north of Manaus	Clean	Wet season	4–37 [†]	0.28 ± 0.13	Ref. (12)
		Dry season	27–334 [†]	0.07 ± 0.06	Ref. (12)
Ground-based site (pasture), southwestern Amazon, Rondonia	Clean	Wet season	16–86 [†]	0.26 ± 0.04	Ref. (13)
	Polluted	Dry season	19–418 [†]	0.37 ± 0.06	Ref. (13)

Table S5. Apparent yields of 2-methyltetrols from isoprene photooxidation under polluted environments. The apparent yield is calculated as $[2\text{-Methyltetrols}]_{\text{particle}}/[\text{Isoprene}]$. Results are listed for each week of sampling. The quantity appearing after “±” indicates the one-sigma variation during the sampling period. Related notes about concentration appear in the caption of Table S2. The apparent yield assumes that all 2-methyltetrols result from isoprene photooxidation (i.e., no primary emissions of 2-methyltetrols) The calculation corresponds to noontime conditions at the equator for OH and O₃ concentrations representative of pollution (cf. Table S3). Noontime 2-methyltetrols and isoprene concentrations were used (i.e., concentrations of 11:20-12:20 and 12:30-13:30). $[2\text{-Methyltetrols}]_{\text{particle}}$ were calculated based on the average particle fractions of 2-methylthreitol and 2-methylerythritol (0.31 and 0.55, respectively) in the wet season of the central Amazon (5). Isoprene concentrations were taken from Batista et al. (1).

	Noontime $[2\text{-Methyltetrols}]_{\text{particle}}$ (ng m ⁻³)		Noontime [Isoprene] (ppb)		Apparent Yield	
	P	S	P	S	P	S
Week 1	67 ± 1	54 ± 2	4.8 ± 0.9	1.7 ± 0.3	0.3%	0.6%
Week 2	56 ± 4	296 ± 89	5.4 ± 1.4	4.2 ± 2.6	0.2%	1.3%
Week 3	142 ± 107	214 ± 8	6.4 ± 0.9	5.6 ± 1.3	0.4%	0.7%
Week 4	267 ± 127	402 ± 110	6.2 ± 0.5	3.2 ± 1.6	0.8%	2.2%
Ensemble Mean					0.4 ± 0.3%	1.2 ± 0.8%

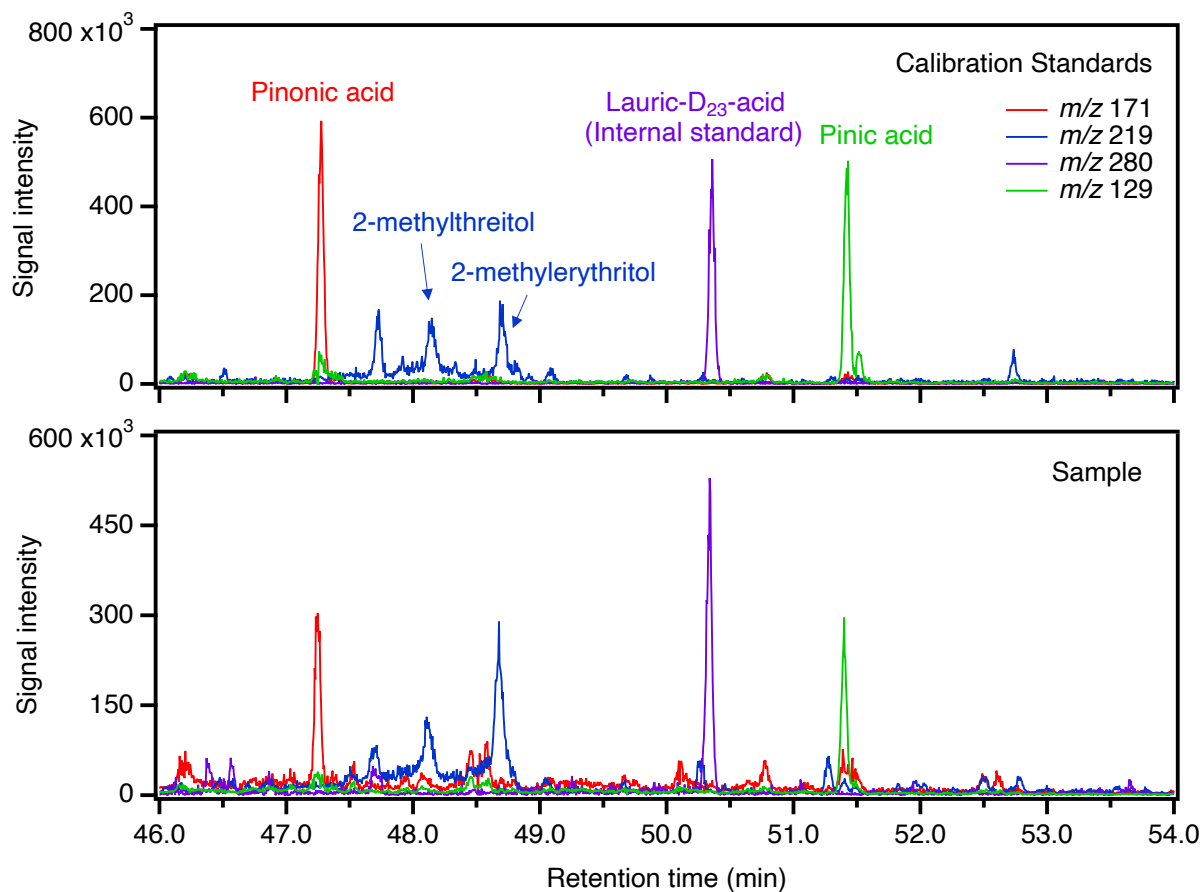


Fig. S1. Examples of chromatograms of standards and samples. The signal intensity at m/z 219 was used for quantification of the concentrations of 2-methylthreitol and 2-methylerythritol, at m/z 171 for the concentration of pinonic acid, at m/z 129 for the concentration of pinic acid, and at m/z 280 for the concentration of lauric-D₂₃-acid.

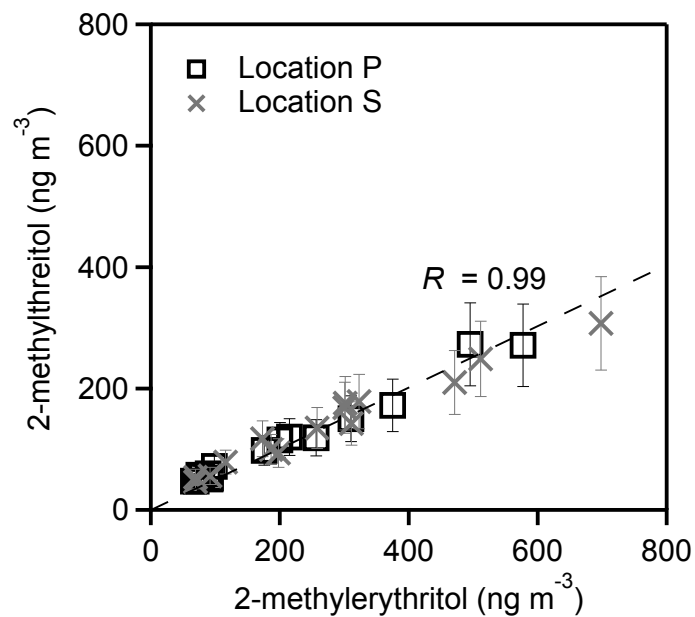


Fig. S2. Relationship between 2-methylthreitol and 2-methylerythritol concentrations. For locations P and S, the two correlation coefficients are both 0.99. Table S2 lists the plotted values.

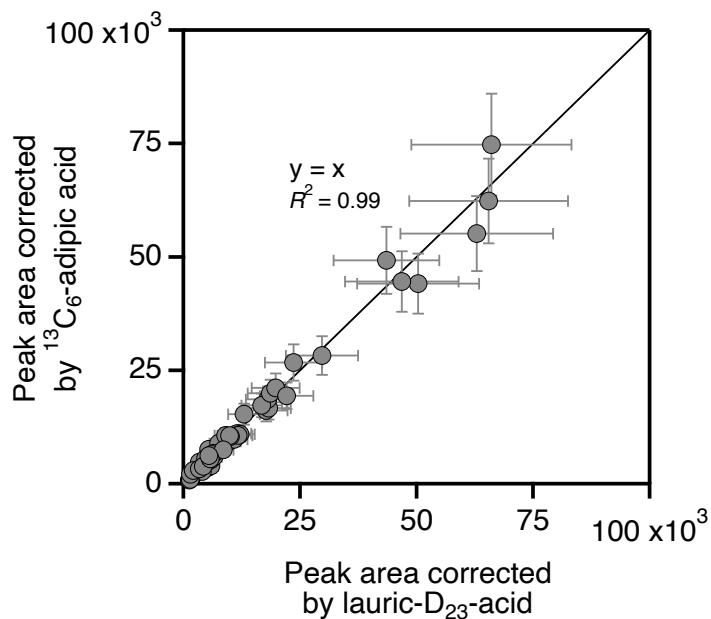


Fig. S3. GC-MS signal correction with different internal standards. Chromatograph peak areas of the five targeted SV-OVOCs in the standard solutions corrected by ¹³C₆-adipic acid are plotted as a function of those corrected by lauric-D₂₃-acid. Figure S1 (top panel) shows an example of a chromatograph of the targeted SV-OVOCs. Standard solutions with SV-OVOC concentrations of 5, 10, 15, and 20 μM were used. Each data point represents a replicate of three. ¹³C₆-adipic acid and lauric-D₂₃-acid were internal standards for the thermal desorption and derivatization, which were injected into the sorbent cartridge before chemical analysis. These standards accounted for any system drift and run-to-run variation. The MSTFA derivatives of the two isotope internal standards represent different categories of volatility. Peak areas corrected by lauric-D₂₃-acid and ¹³C₆-adipic acid follow the 1:1 line, demonstrating the effectiveness of thermal-desorption and derivatization for target SV-OVOCs during the analysis.

REFERENCES

1. C. E. Batista, J. Ye, I. O. Ribeiro, P. C. Guimarães, A. S. S. Medeiros, R. G. Barbosa, R. L. Oliveira, S. Duvoisin, K. J. Jardine, D. Gu, A. B. Guenther, K. A. McKinney, L. D. Martins, R. A. F. F. Souza, S. T. Martin, S. Duvoisin Jr, Intermediate-scale horizontal isoprene concentrations in the near-canopy forest atmosphere and implications for emission heterogeneity. *Proceedings of the National Academy of Sciences of the United States of America* **116**, 19318-19323 (2019).
2. F. Santos, K. Longo, A. Guenther, S. Kim, D. Gu, D. Oram, G. Forster, J. Lee, J. Hopkins, J. Brito, S. Freitas, Biomass burning emission disturbances of isoprene oxidation in a tropical forest. *Atmospheric Chemistry and Physics* **18**, 12715-12734 (2018).
3. T. M. Butler, D. Taraborrelli, C. Brühl, H. Fischer, H. Harder, M. Martinez, J. Williams, M. G. Lawrence, J. Lelieveld, Improved simulation of isoprene oxidation chemistry with the ECHAM5/MESSy chemistry-climate model: lessons from the GABRIEL airborne field campaign. *Atmospheric Chemistry and Physics* **8**, 4529-4546 (2008).
4. T. Cui, Z. Zeng, E. O. dos Santos, Z. Zhang, Y. Chen, Y. Zhang, C. A. Rose, S. H. Budisulistiorini, L. B. Collins, W. M. Bodnar, R. A. F. de Souza, S. T. Martin, C. M. D. Machado, B. J. Turpin, A. Gold, A. P. Ault, J. D. Surratt, Development of a hydrophilic interaction liquid chromatography (HILIC) method for the chemical characterization of water-soluble isoprene epoxydiol (IEPOX)-derived secondary organic aerosol. *Environmental Science: Processes & Impacts* **20**, 1524-1536 (2018).
5. G. Isaacman-VanWertz, L. D. Yee, N. M. Kreisberg, R. Wernis, J. A. Moss, S. V. Hering, S. S. De Sá, S. T. Martin, M. L. Alexander, B. B. Palm, W. Hu, P. Campuzano-

- Jost, D. A. Day, J. L. Jimenez, M. Riva, J. D. Surratt, J. Viegas, A. Manzi, E. Edgerton, K. Baumann, R. Souza, P. Artaxo, A. H. Goldstein, Ambient gas-particle partitioning of tracers for biogenic oxidation. *Environmental Science & Technology* **50**, 9952-9962 (2016).
6. H. K. Lam, K. C. Kwong, H. Y. Poon, J. F. Davies, Z. Zhang, A. Gold, J. D. Surratt, M. N. Chan, Heterogeneous OH oxidation of isoprene-epoxydiol-derived organosulfates: kinetics, chemistry and formation of inorganic sulfate. *Atmospheric Chemistry and Physics* **19**, 2433-2440 (2019).
7. R. Atkinson, J. Arey, Atmospheric degradation of volatile organic compounds. *Chemical Reviews* **103**, 4605-4638 (2003).
8. S. H. Kessler, J. D. Smith, D. L. Che, D. R. Worsnop, K. R. Wilson, J. H. Kroll, Chemical sinks of organic aerosol: kinetics and products of the heterogeneous oxidation of erythritol and levoglucosan. *Environmental Science & Technology* **44**, 7005-7010 (2010).
9. M. Claeys, B. Graham, G. Vas, W. Wang, R. Vermeylen, V. Pashynska, J. Cafmeyer, P. Guyon, M. O. Andreae, P. Artaxo, W. Maenhaut, Formation of secondary organic aerosols through photooxidation of isoprene. *Science* **303**, 1173-1176 (2004).
10. Y. Liu, R. Seco, S. Kim, A. B. Guenther, A. H. Goldstein, F. N. Keutsch, S. R. Springston, T. B. Watson, P. Artaxo, R. A. F. Souza, K. A. McKinney, S. T. Martin, Isoprene photo-oxidation products quantify the effect of pollution on hydroxyl radicals over Amazonia. *Science Advances* **4**, eaar2547 (2018).
11. L. D. Yee, G. Isaacman-VanWertz, R. A. Wernis, N. M. Kreisberg, M. Glasius, M. Riva, J. D. Surratt, S. S. de Sá, S. T. Martin, M. L. Alexander, B. B. Palm, W. Hu, P.

- Campuzano-Jost, D. A. Day, J. L. Jimenez, Y. Liu, P. K. Misztal, P. Artaxo, J. Viegas, A. Manzi, R. A. F. de Souza, E. S. Edgerton, K. Baumann, A. H. Goldstein, Natural and anthropogenically influenced isoprene oxidation in Southeastern United States and Central Amazon. *Environmental Science & Technology* **54**, 5980-5991 (2020).
12. N. J. D. González, A. K. Borg-Karlson, P. Artaxo, A. Guenther, R. Krejci, B. Nozière, K. Noone, Primary and secondary organics in the tropical Amazonian rainforest aerosols: chiral analysis of 2-methyltetraols. *Environmental Science: Processes & Impacts* **16**, 1413-1421 (2014).
13. M. Claeys, I. Kourtchev, V. Pashynska, G. Vas, R. Vermeylen, W. Wang, J. Cafmeyer, X. Chi, P. Artaxo, M. O. Andreae, W. Maenhaut, Polar organic marker compounds in atmospheric aerosols during the LBA-SMOCC 2002 biomass burning experiment in Rondônia, Brazil: sources and source processes, time series, diel variations and size distributions. *Atmospheric Chemistry and Physics* **10**, 9319-9331 (2010).